Fermi Contours and Adsorbate Periodicities: O/Mo(011) and O/W(011)

S. Dhar, Kevin E. Smith,* S. D. Kevan†
Physics Department, University of Oregon, Eugene, Oregon 97403
(Received 26 April 1994)

We present experimental Fermi contours for surface-localized states on O/Mo(011) and O/W(011). The contours are consistent with the fact that a (2 × 2) superstructure is observed on Mo(011) but not on W(011) through a global Fermi contour instability in which entire orbits are closely coupled by the wave vector of the superlattice. Our results are also consistent with a recently observed sevenfold reconstruction of the (2 × 2) oxygen structure on Mo(011) through a simple Peierls mechanism. We discuss the generality of such behavior in adsorption systems.

PACS numbers: 79.60.Dp, 73.20.At, 82.65.My

One of the most commonly observed yet most poorly understood phenomena in modern surface chemical physics concerns the lateral potential energy surfaces which conspire to produce the variety of observed superlattice periodicities in adsorbed layers. The source of this difficulty is the substrate itself since this mediates the lateral interactions in a complex way. While useful empirical models for substrate-mediated interactions have existed for over 20 years [1–10], a precise, nearly first principles characterization of these on an energy scale relevant to most surface processes has not been available [11]. It is thus of interest to examine the adsorbate superstructure periodicity problem from the perspective of other experimentally accessible surface characteristics to try to deduce the relevant interactions. One of the empirical models, which is relevant to metal surfaces, utilizes the existence of well-defined Fermi contours. These support Friedel-like oscillations that lead to an oscillatory lateral interaction potential [12]. In the present Letter, we report experimentally determined surface Fermi contours for ordered oxygen layers on Mo(011) and W(011), and show that they provide a mechanism to explain some of the remarkable qualitative differences observed in the low-coverage phase diagrams for these systems.

The well-studied temperature-coverage phase diagrams for oxygen adsorbed onto Mo(011) and W(011) provide an excellent example of the precision with which lateral potentials can be deduced but the imprecision with which they are understood. These systems have been extensively studied experimentally [13–19] and have thus provided models upon which to apply a battery of modern lattice gas statistical techniques [20–23]. While these are similar metals and have many similar bulk and surface properties, there are substantial differences in the phase diagrams for these two adsorbate systems. O/W(011) exhibits three ordered phases: a (2 × 1) phase at 0.5 monolayer, a (2 × 2) phase at 0.75 monolayer, and a (1 × 1) phase at full monolayer coverage. The (2 × 1) phase is also observed for O/Mo(011), but there is also a (2 × 2) phase observed at 0.25 monolayer, and a corresponding (2 × 2) phase is not observed at 0.75 monolayer. Complex patterns including a sevenfold reconstruction are observed near 0.3 monolayer for O/Mo(011) [18,19], but not on W(011). In both systems, the low-coverage ordered phases are observed well below the "correct" nominal coverage, suggesting the prevalence of attractive lateral interactions even for nearest-neighbor sites. Both phase diagrams exhibit serious asymmetries about half monolayer coverage. In lattice gas theory this implies nonpairwise additive interactions [3,4], although other shortcomings of the lattice gas model, such as the assumption of harmonic forces binding atoms to a particular site and the discretizing of the interaction potential itself, can also lead to such behavior [24,25]. The phase diagrams have been modeled in terms of a small number of lattice gas energies, but the underlying source of most of these interactions is not well understood. Despite their obvious strengths, these efforts serve to distinguish the two primary shortcomings of such theories. Specifically, one does not *a priori* know which interactions to include, and one has no real insight in interpreting the derived lattice gas interaction energies.

The Fermi contours for surface-localized states were measured with angle-resolved photoemission (ARP) using techniques similar to those reported elsewhere [26,27]. Experiments were performed at the National Synchrotron Light Source at Brookhaven National Laboratory using an apparatus which has been described previously [28,29]. Experimental energy and angular resolutions were ~100 meV and <1° full width at half maximum, respectively. Figure 1 shows a typical set of ARP spectra collected from Mo(011)-(2 × 2)O along the $\bar{\Delta}$ line in the surface Brillouin zone (SBZ). The dominant spectral feature disperses upward in energy with increasing parallel wave vector, $k_{\parallel}$, and eventually crosses the Fermi level, E_F, near $k_{\parallel} = 0.95$ Å^{-1}. This crossing represents a single point labeled "*A*" along the $\bar{\Delta}$ line in the SBZ, as shown in Fig. 2. The spectral feature exhibits the two behaviors typical of surface states and resonances, that is, its sensitivity to contamination discussed below and its lack of dispersion with momentum normal to the surface. More

0031-9007/94/73(10)/1448(4)$06.00

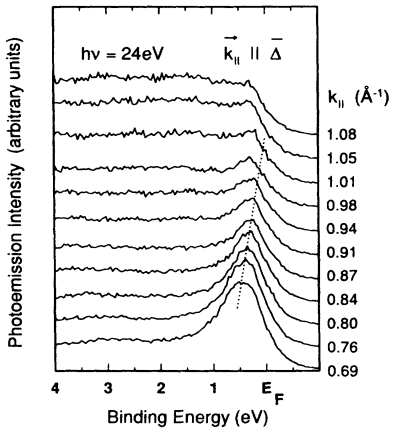

FIG. 1. ARP energy distribution curves for the Mo(011)-(2 × 2)O system at 0.25 monolayer coverage collected at a photon energy of 24 eV. The detector was situated in the (01$\bar{1}$) or $\bar{\Delta}$ mirror plane of the SBZ, which cuts one of the elliptical Fermi contours near $k_{\parallel} = 0.95$ Å^{-1}. Note the dispersion of the primary spectral feature, a pure surface state, across E_F near this wave vector.

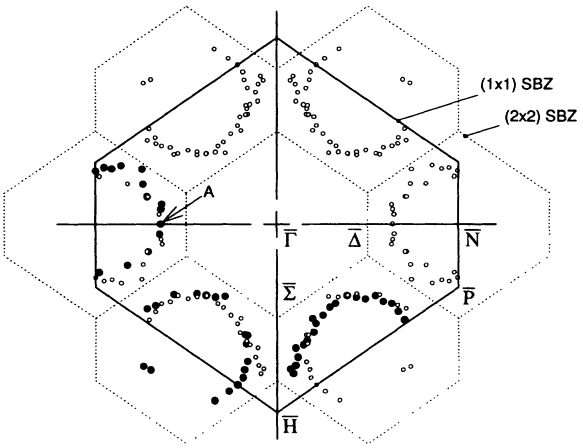

FIG. 2. Measured surface Fermi contours for Mo(011)-(2 × 2)O at a coverage of 0.25 monolayer. Filled circles are points measured using spectra similar to those in Fig. 1, while open circles are produced by mirror symmetry operations in the SBZ. Note the existence of two elliptical hole orbits of very nearly the same dimension centered along the edges of the (1 × 1) SBZ. Also shown are the (2 × 2) SBZ boundaries in which both orbits are centered.

importantly, there is no ambiguity in assigning it to be an intrinsic surface state at E_F since the point A lies outside the projection of the experimentally determined bulk Mo Fermi surface [27]. At this point the band necessarily lies in a projected bulk band gap and point A lies on a true 2D surface Fermi contour. Crossings such as this could be located with a precision of ~0.02 Å^{-1}, albeit with somewhat reduced accuracy due to the difficulty of determining exactly where the spectral feature crosses E_F (see Fig. 1).

Collection of many ARP spectra throughout the SBZ allows direct determination of 2D Fermi contours, both for the clean surface and upon oxygen adsorption. On the clean surface, four closed contours were previously observed on both W(011) [26] and Mo(011) [27]: three small, elliptical hole pockets located at the center and along the two edges of the SBZ and a larger, irregular electron pocket also centered in the SBZ. The three hole pockets are all extinguished upon oxygen exposure. That is, the band which forms these is apparently greatly altered by chemisorption bond formation so that it is shifted downward in energy and its Fermi segments disappear. By contrast, the band forming the electron pocket is pulled only slightly downward in energy upon oxygen adsorption. The pocket thus grows until it merges with its images in the neighboring SBZ's to form two nearly elliptical hole pockets along the edges of the SBZ.

As shown in Fig. 2, at 0.25 monolayer coverage these two pockets are nearly the same size and shape, although there is no reason by symmetry why this needs to be the case. The hole pockets are centered in the (2 × 2) superlattice Brillouin zones, shown as dotted lines in Fig. 2. This situation implies what might be called a "global" Peierls distortion [30]. Unlike a typical Peierls distortion where only a small segment of Fermi surface or contour is coupled to its image, each point on one of these two contours has a tangent which is parallel to the tangent of a point on the other contour, and these two points are separated by very nearly a reciprocal lattice vector for the (2 × 2) net. This provides a logical and purely electronic driving force for producing a (2 × 2) ordering pattern at 0.25 monolayer for O/Mo(011). The stabilization energy associated with formation of small band gaps around the contour will produce attractive interactions in second-neighbor sites and thus to the tendency to form (2 × 2) islands at low coverage, as observed. An estimate of the magnitude of the gaps can be obtained from the disordering temperature of the (2 × 2) phase of 600 K [18]. The half-gaps would thus be $\sim k_B T_c \sim 60$ meV. The breadth of the spectral feature crossing E_F in Fig. 1 precludes direct observation of these gaps.

By contrast, the Fermi contours do not support such a mechanism for O/W(011), and no low-coverage (2 × 2) phase is observed. Figure 3 shows Fermi contours for W(011)-(2 × 1)O at 0.5 monolayer coverage. In this system, once again the hole pockets on the clean surface are extinguished while the electron pocket grows upon oxygen adsorption. The electron pocket initially merges with its image and then at higher coverage, after the work function change has reversed direction, the contours separate again to leave one electron pocket. At no point are there two hole pockets which are strongly coupled through the global Peierls distortion discussed above. The two symmetry-related SBZ boundaries for

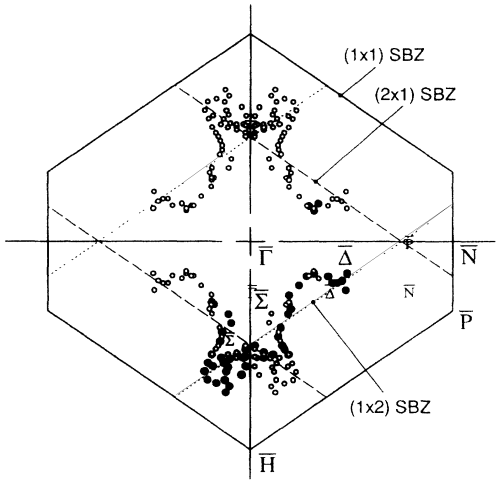

FIG. 3. Experimental surface Fermi contours for W(011)-(2 × 1)O at a coverage of 0.5 monolayer. As in Fig. 2, filled circles are measured points, while open circles are produced by mirror symmetry operations in the SBZ. In this case, the two elliptical hole orbits observed to be centered in (2 × 2) Brillouin zones on Mo(011) are not observed for any coverage. The Fermi contours in this case cross the (2 × 1) SBZ boundaries at which point small wiggles associated with superlattice band gaps are apparent.

the (2 × 1) superstructure are also shown in Fig. 3. Systematic "wiggles" are readily apparent in the contours as they cross these boundaries. These are partially obscured by the inevitable averaging from the two-domain surface. However, a rough estimate of ~30–40 meV for the corresponding energy gaps at E_F can be obtained from a simple application of $\mathbf{k} \cdot \mathbf{p}$ perturbation theory. In principle, one would expect to see sections of the Fermi contours produced by umklapp through these superlattice zone boundaries. That these are not observed is undoubtedly due to the expected weak ARP intensity for such features.

These two data sets thus provide an explanation for at least one of the differences observed between the two phase diagrams. They do not provide any direct rationale for the higher-coverage (2 × 1) and (2 × 2) features in the phase diagrams. These higher-coverage phases all involve placing oxygen atoms on nearest-neighbor sites, and the influence of short-range interactions which are not specifically related to Fermi contours will be correspondingly greater.

Recently, a weaker, longer-range reconstruction of the (2 × 2)O/Mo(011) surface has been observed [19]. In this case, at temperatures below ~200 K, weak seventh-order diffraction spots were observed along the (01$\bar{1}$) or $\bar{\Delta}$ direction. The Fermi contours in Fig. 2 are compatible with such a reconstruction through a normal Peierls distortion. The width of the two hole pockets along $\bar{\Delta}$ is $\sim\frac{5}{14}$ the width of the (1 × 1) SBZ along the $\bar{\Delta}$ direction. The separation of the contour from the (2 × 2) SBZ boundary is thus $\frac{1}{14}$ the (1 × 1) SBZ dimension, a fact which favors sevenfold periodicity. To date, no such long-range reconstruction has been observed for O/W(011), and none is predicted by the data in Fig. 3. It is interesting to speculate upon the generality of such long-range reconstructions which are perhaps driven by screening anomalies. The seventh-order diffraction spots for O/Mo(011) are quite weak and their observation required, in addition to operation below room temperature, a low energy electron diffraction system optimized for single particle detection. The fact that other similar reconstructions have not been observed thus does not mean that they do not exist. However, this system may be nearly optimal for such a reconstruction. The oxygen atoms adsorb in or near the long-bridge site where the restoring force for displacements along the (01$\bar{1}$) direction is small. A correspondingly small electronic screening anomaly would lead to reconstruction.

An important aspect of the lateral interaction problem is that relatively weak interactions have a pronounced impact on the properties of an adsorbed layer. This is particularly true of regions of attractive interaction potential. In lattice gas theory, for example, an attractive site interaction energy of ~100 K will have a pronounced impact upon kinetic and thermodynamic properties at temperatures of several hundred kelvin. 100 K corresponds to an energy of 8 meV, which on the scale of chemical bonding energies, is very small. This sensitivity of macroscopic properties to weak energetic interactions places great demands on the accuracy of first principles calculations which propose to examine the lateral interaction potential energy surface between adsorbed atoms or molecules. More importantly, even the relatively weak and rapidly decaying oscillatory through surface interactions discussed above can play a major role in the properties of the adsorbed film. Finally, the energetics of a Fermi-contour-driven ordering pattern cannot in any simple way be separated into discrete, pairwise additive lattice gas energies. This nonpair behavior is typical of metallic cohesion in general and should thus not be surprising.

This work was carried out in part at the NSLS at Brookhaven National Laboratory which is supported by the U.S. Department of Energy, Division of Materials Science and Division of Chemical Sciences. Financial support from the U.S. DOE under Grant No. DE-FG06-86ER45275 is gratefully acknowledged.

*Present address: To whom correspondence should be addressed. Current address: Physics Department, Boston University, Boston, MA 02215.
†Electronic address: kevan@oregon.uoregon.edu

[1] T. B. Grimley, Proc. R. Soc. London **90**, 751 (1967).
[2] T. L. Einstein and J. R. Schrieffer, Phys. Rev. B **7**, 3629 (1973).

[3] T. L. Einstein in, *Chemistry and Physics of Solid Surfaces*, edited by R. Vanselow (CRC, Boca Raton, FL, 1979).
[4] T. L. Einstein, Langmuir **7**, 2520 (1991).
[5] K. H. Lau and W. Kohn, Surf. Sci. **75**, 69 (1978).
[6] N. H. March, Prog. Surf. Sci. **25**, 229 (1987).
[7] J. Muscat, Prog. Surf. Sci. **25**, 211 (1987).
[8] P. Johansson, Solid State Commun. **31**, 591 (1979).
[9] A. C. Redfield and A. Zangwill, Phys. Rev. B **46**, 4289 (1992).
[10] A. M. Bradshaw and M. Scheffler, J. Vac. Sci. Technol. **16**, 447 (1979).
[11] P. J. Feibelman, Annu. Rev. Phys. Chem. **40**, 261 (1989).
[12] J. Friedel, Adv. Phys. **3**, 446 (1954).
[13] G.-C. Wang, T.-M. Lu, and M. G. Lagally, J. Chem. Phys. **69**, 479 (1978).
[14] E. Bauer, H. Poppa, and Y. Viswanath, Surf. Sci. **58**, 517 (1976).
[15] E. Bauer and T. Engel, Surf. Sci. **71**, 695 (1978).
[16] E. Bauer and H. Poppa, Surf. Sci. **88**, 31 (1979).
[17] E. Bauer and H. Poppa, Surf. Sci. **127**, 243 (1983).
[18] W. Witt and E. Bauer, Ber. Bunsen-Ges. Phys. Chem. **90**, 248 (1986).
[19] K. Grzelakowski, I. Lyuksyutov, and E. Bauer, Surf. Sci. **216**, 472 (1989).
[20] Y. W. Ching, D. L. Huber, M G. Lagally, and G.-C. Wang, Surf. Sci. **77**, 550 (1978).
[21] K. Kaski, W. Kinzel, and J. D. Gunton, Phys. Rev. B **27**, 6777 (1983).
[22] P. A. Rikvold, K. Kaski, J. D. Gunton, and M. C. Yalabik, Phys. Rev. B **29**, 6285 (1984).
[23] B. Dünweg, A. Milchev, and P. A. Rikvold, J. Chem. Phys. **94**, 3958 (1991).
[24] B. N. J. Persson, Solid State Commun. **70**, 215 (1989).
[25] B. N. J. Persson, Solid State Commun. **70**, 211 (1989).
[26] R. H. Gaylord, K. Jeong, and S. D. Kevan, Phys. Rev. Lett. **62**, 203 (1989).
[27] K. Jeong, R. H. Gaylord, and S. D. Kevan, Phys. Rev. B **39**, 2973 (1989).
[28] P. Thiry *et al.*, Nucl. Instrum. Methods Phys. Res. **222**, 85 (1984).
[29] S. D. Kevan, Rev. Sci. Instrum. **54**, 1441 (1983).
[30] R. E. Peierls, *Quantum Theory of Solids* (Clarendon, Oxford, 1964).